Bell-state tomography in a silicon many-electron artificial molecule

Ross C. C. Leon,[1,*] Chih Hwan Yang,[1] Jason C. C. Hwang,[1,†] Julien Camirand Lemyre,[2]
Tuomo Tanttu,[1] Wei Huang,[1] Jonathan Y. Huang,[1] Fay E. Hudson,[1] Kohei M. Itoh,[3]
Arne Laucht,[1] Michel Pioro-Ladrière,[2,4] Andre Saraiva,[1,‡] and Andrew S. Dzurak[1,§]

[1] *School of Electrical Engineering and Telecommunications,
The University of New South Wales, Sydney, NSW 2052, Australia.*
[2] *Institut Quantique et Département de Physique,
Université de Sherbrooke, Sherbrooke, Québec J1K 2R1, Canada*
[3] *School of Fundamental Science and Technology, Keio University,
3-14-1 Hiyoshi, Kohokuku, Yokohama 223-8522, Japan.*
[4] *Quantum Information Science Program, Canadian Institute for Advanced Research, Toronto, ON, M5G 1Z8, Canada*

arXiv:2008.03968

- FAM talk -

Florian Froning
11.09.2020

Introduction

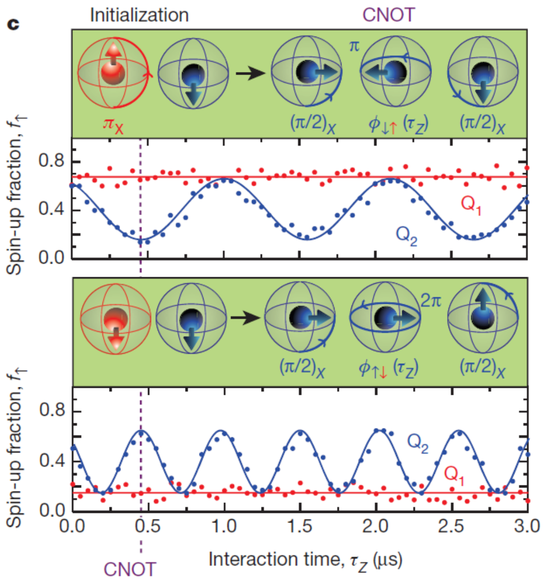

Two-Qubit Logic

Veldhorst, M. *et al. Nature* **526**, 410–414 (2015)

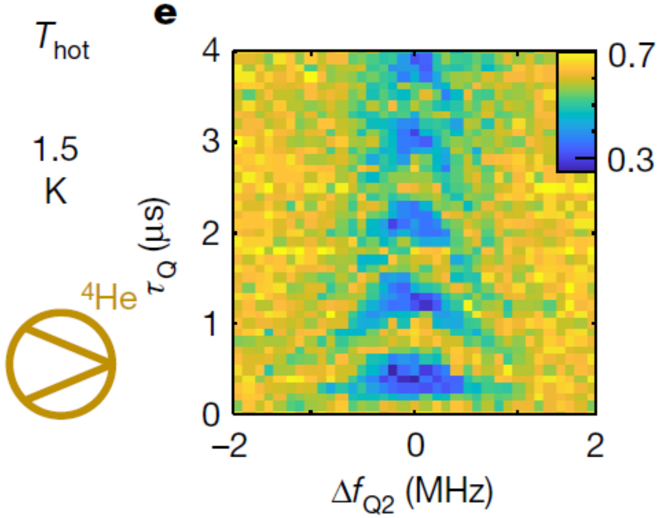

Hot Qubit

- 1.5 K

Yang, C. H. *et al. Nature* **580**, 350–354 (2020)

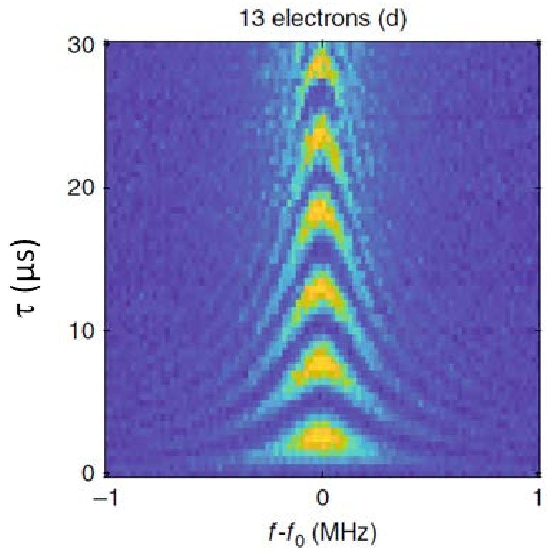

High Occupation Qubit

- single qubit gates
- f_{Rabi} tunability

Leon, R. C. C. *et al. Nat Commun.* **11**, 797 (2020)

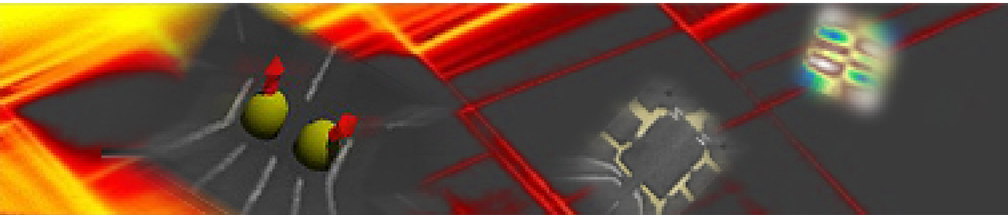

Motivation: Higher Orbitals

- Orbitals play a major role in performance and operation of spin qubits
  - $W_{rel} \propto 1/E_{orb}^{4}$
  - $f_{Rabi} \propto 1/E_{orb}^{2}$

- larger size of multielectron wavefunctions can
  - enable higher control fidelities
  - enhance exchange coupling between qubits

- screening of disorder by increased electron density

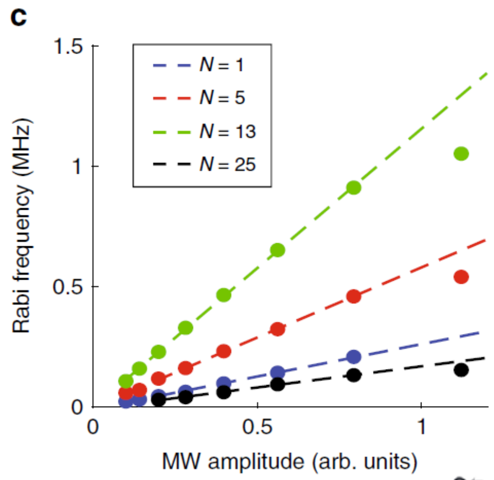

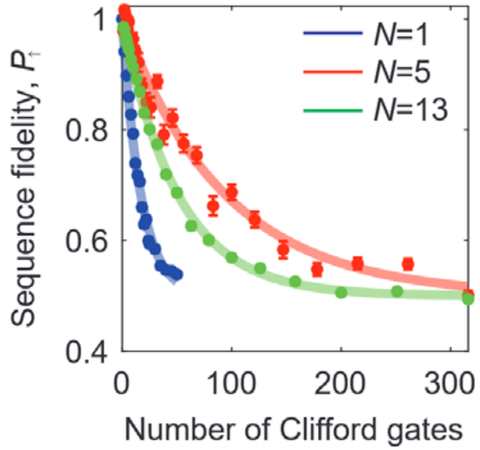

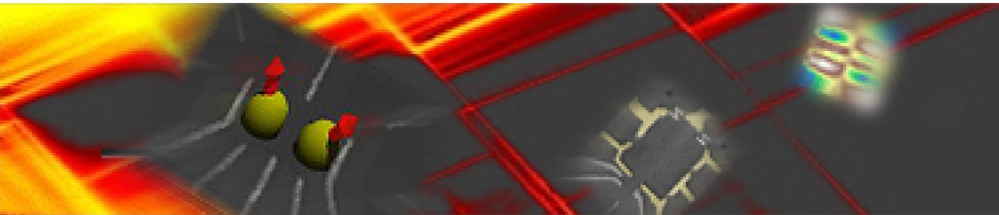

Leon, R. C. C. *et al.*, *Nat Commun.* **11**, 797 (2020)
Camenzind, L. C. *et al.*, *Phys. Rev. Lett.* **122**, 207701 (2019)

Device

- **Si-MOS** QD with Co **micromagnet** for spin manipulation and **SET** for charge readout

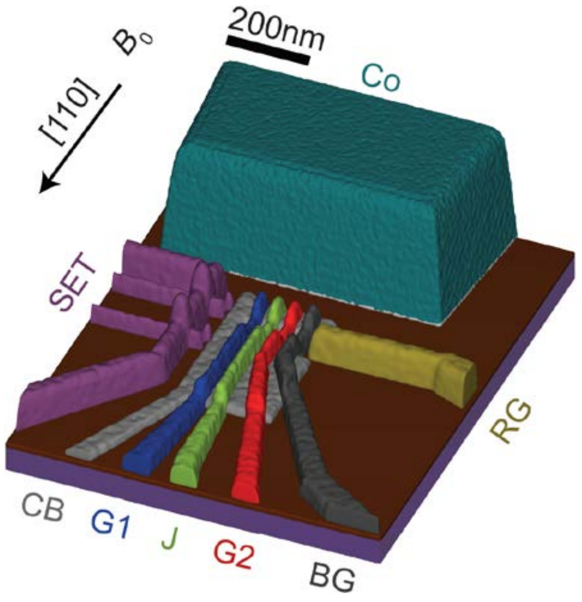

Fig: 3D visualization of the device

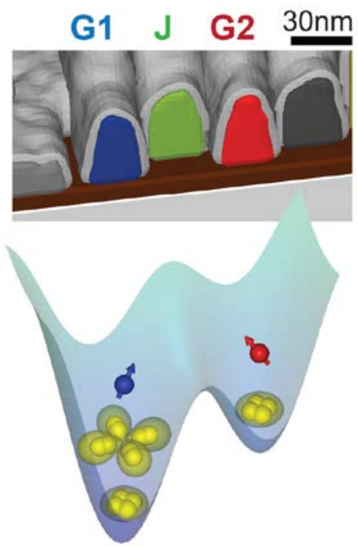

Fig: Occupation of the dot in the (13,5) charge configuration

- multiple electrons: shell-filling [1]
- load a total of 18 electrons, then decouple DQD from reservoir
- (12,6)-(13,5) transition (effective (1,1) occupation)
- B_0 = 1 T

✓ single-qubit operation [1]

❑ two-qubit operation

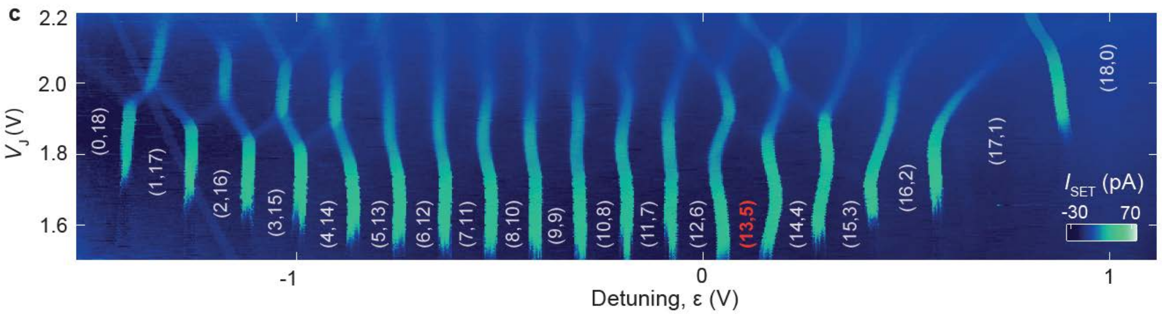

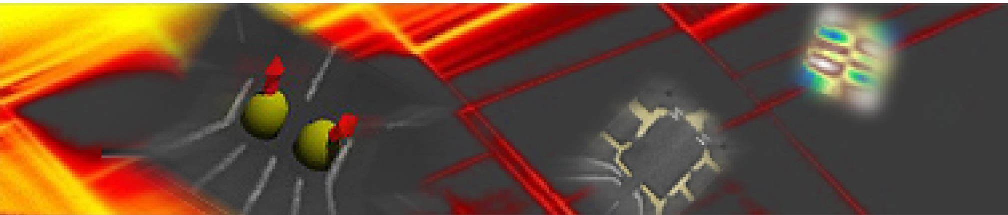

[1] Leon, R. C. C. *et al. Nat Commun* **11**, 797 (2020)

Outline

Single-Qubit

CZ gate

Bell state tomography

Summary

Stark shift

- nonlinear dependence of qubit resonance frequency (Stark shift)
- color code: efficiency of the adiabatic inversion of the spins

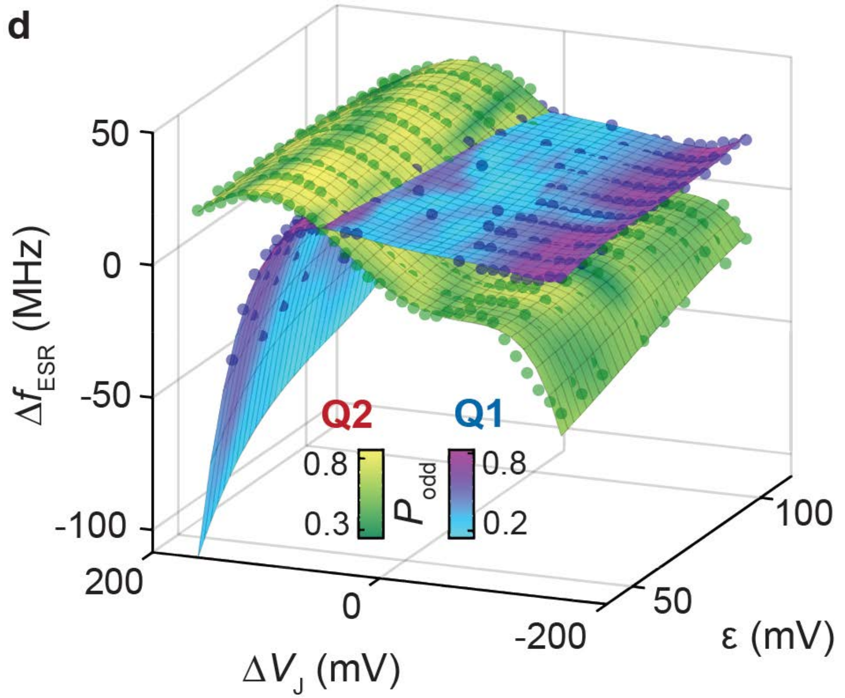

Fig: Resonance frequency as a function of ε and V_J

Outline

- Single-Qubit
- CZ gate
- Bell state tomography
- Summary

Two-Qubit Gates

- require sizeable exchange interaction for fast exchange oscillation
  - provided by higher orbitals in contrast to (1,1) charge configuration
- but: single qubit gates require low exchange coupling for high gate fidelity

- here: two methods to control exchange coupling

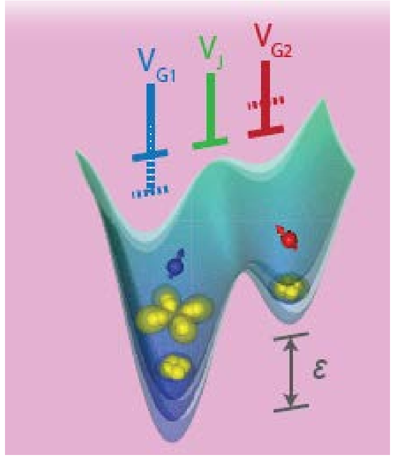

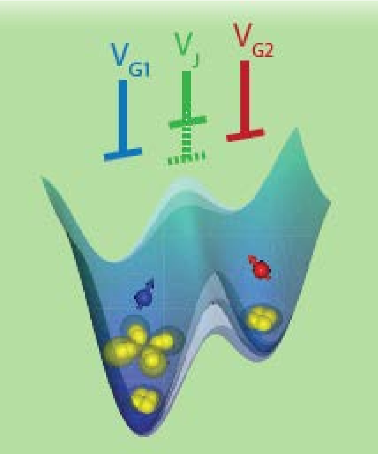

Ramsey type measurement

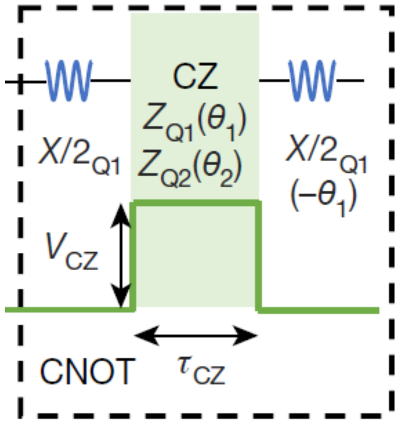

CZ Gate

Detuning Control | **J Control**

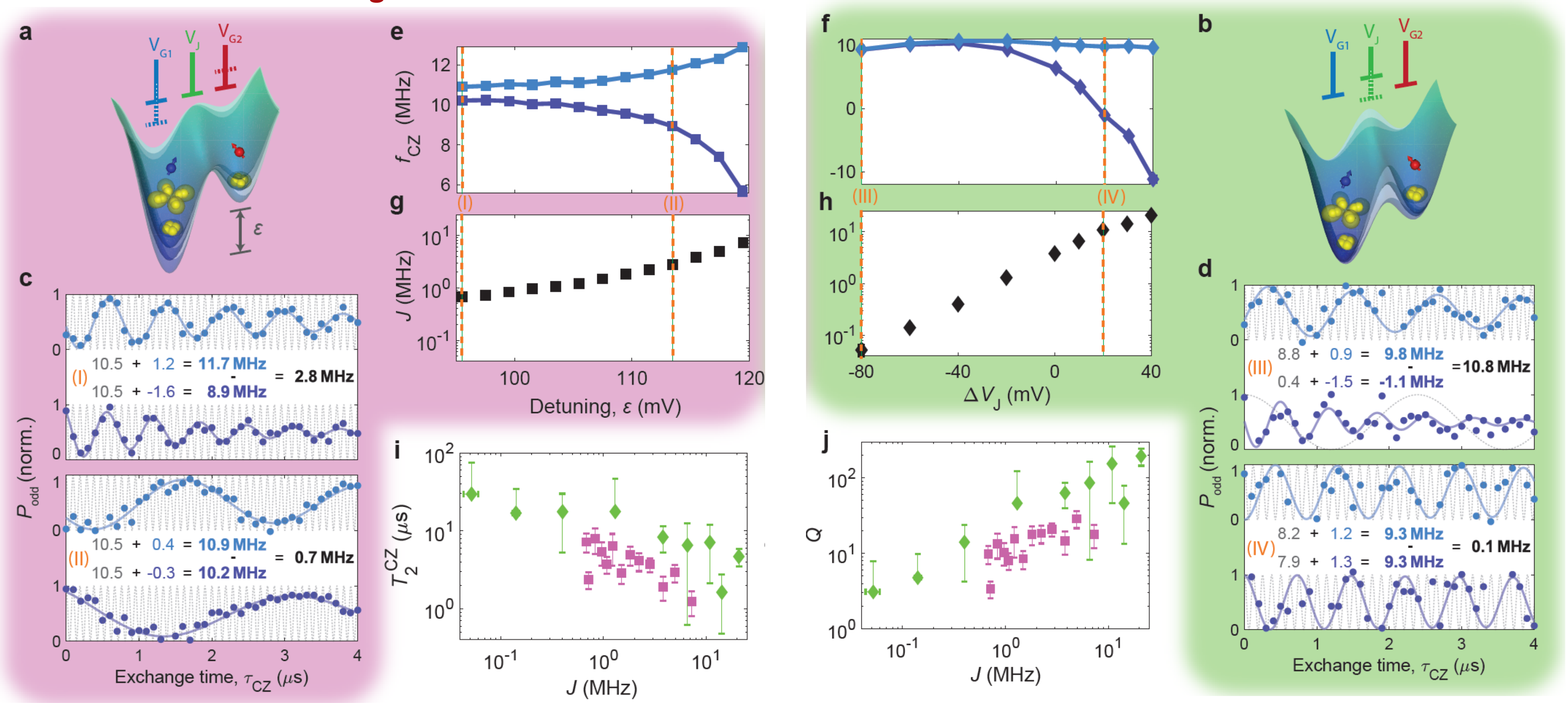

Two-Qubit Clifford Space

- single qubit gates together with CZ gate
- but: Stark shift requires different operation points of high-fidelity single qubit gates
  - inhibits dynamical decoupling

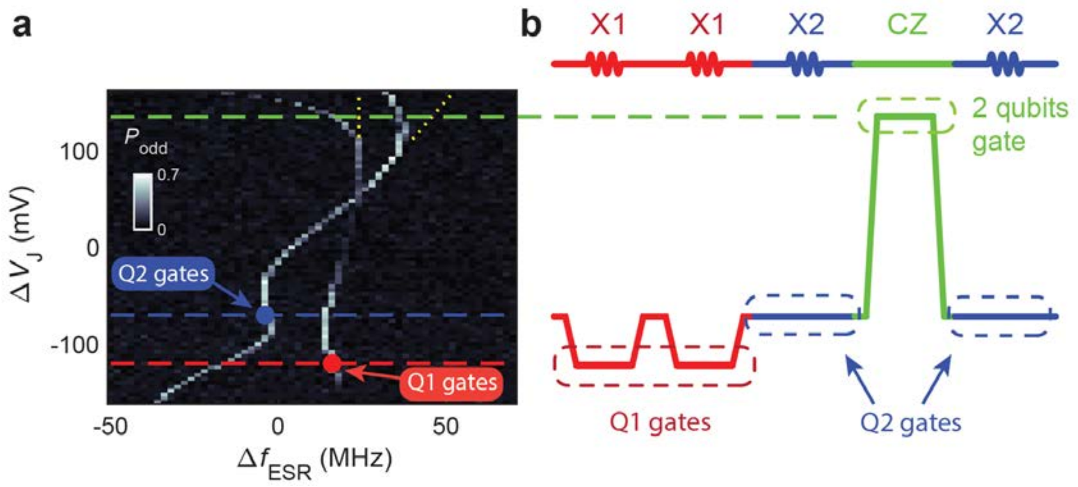

Outline

1. Single-Qubit
2. CZ gate
3. Bell state tomography
4. Summary

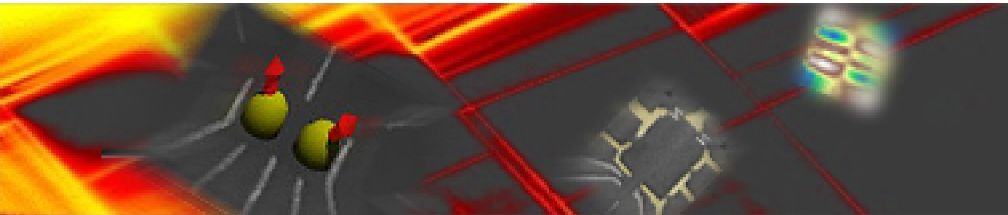

Bell-State Tomography

$$\textbf{(d)}\ \Phi^+ = \frac{|\uparrow\uparrow\rangle + |\downarrow\downarrow\rangle}{\sqrt{2}},\ \textbf{(e)}\ \Phi^- = \frac{|\uparrow\uparrow\rangle - |\downarrow\downarrow\rangle}{\sqrt{2}},\ \textbf{(f)}\ \Psi^+ = \frac{|\uparrow\downarrow\rangle + |\downarrow\uparrow\rangle}{\sqrt{2}},\ \textbf{(g)}\ \Psi^- = \frac{|\uparrow\downarrow\rangle - |\downarrow\uparrow\rangle}{\sqrt{2}}$$

$(87.1 \pm 2.8)\,\%$, $(90.3 \pm 3.0)\,\%$, $(90.3 \pm 2.4)\,\%$ and $(90.2 \pm 2.9)\,\%$

Bell state fidelities compare favorably

Huang, W. et al., Nature 569, 532–536 (2019)	Ψ^+	80 % ± 0.6 %
	Ψ^-	82 % ± 0.6 %
	Φ^+	89 % ± 0.6 %
	Φ^-	89 % ± 0.6 %
Watson, T. F. *et al., Nature* **555**, 633–637 (2018)	Ψ^+	88 % ± 2 %
	Ψ^-	88 % ± 2 %
	Φ^+	85 % ± 2 %
	Φ^-	89 % ± 2 %

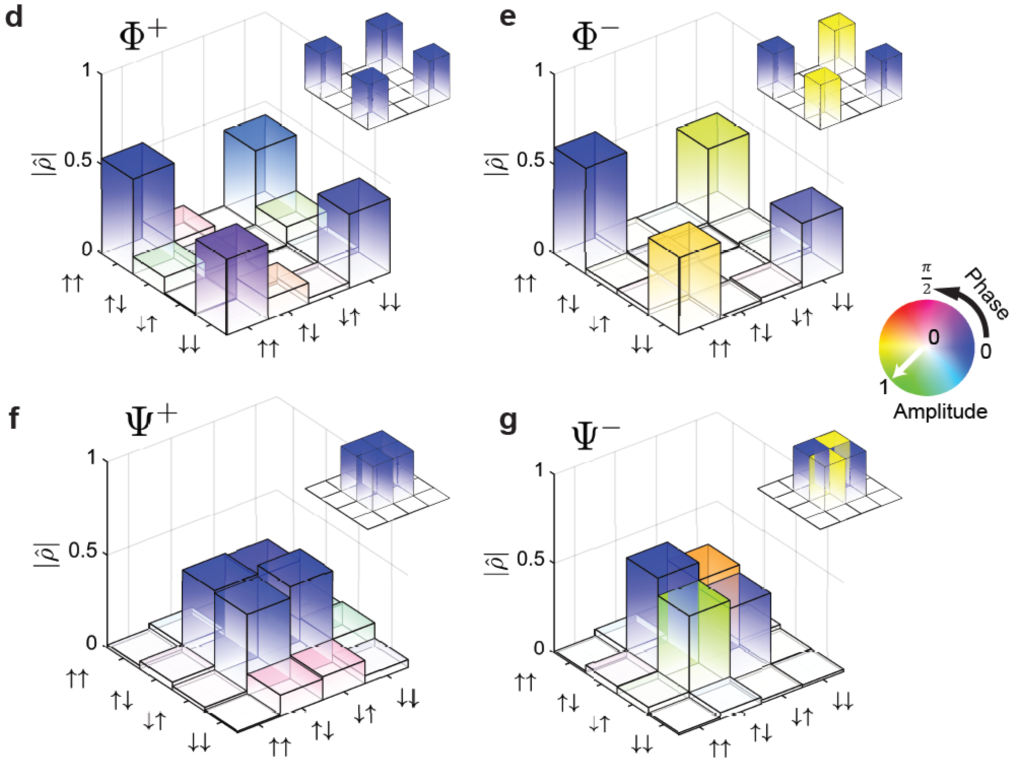

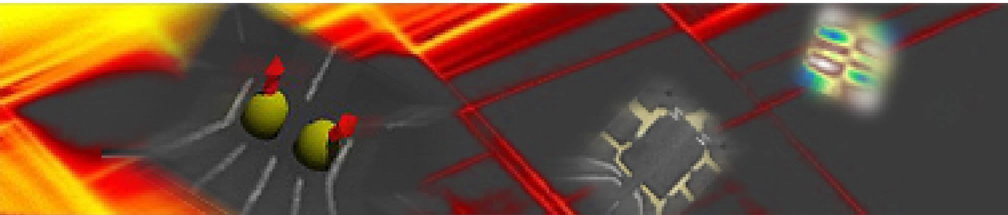

Outline

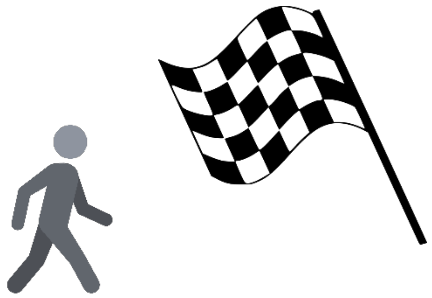

- Single-Qubit
- CZ gate
- Bell state tomography
- Summary

Summary and Outlook

- multielectron qubits
  - efficient single-qubit gates
  - exchange coupling which can be used for two-qubit gates
- exchange coupling control via plunger gates or interdot tunnel barrier
- Bell state fidelities compare favorably
- but: unability to refocus idling spins

Parity Readout

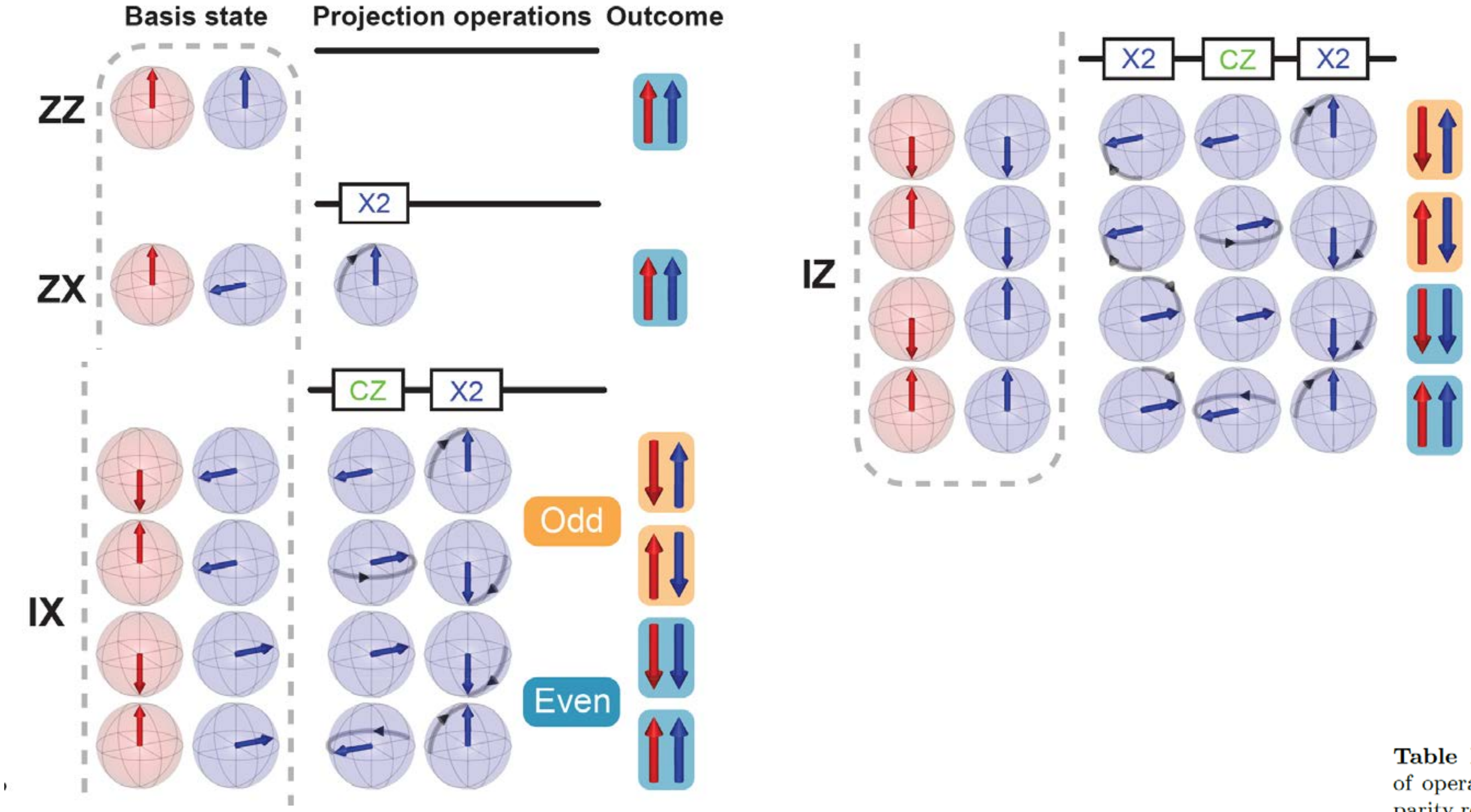

Projection	Operations
ZZ	I
YZ	X1
XZ	Y1
ZY	X2
ZX	Y2
YY	X1–X2
YX	X1–Y2
XY	Y1–X2
XX	Y1–Y2
YI	CZ–X1
XI	CZ–Y1
IY	CZ–X2
IX	CZ–Y2
ZI	X1–CZ–X1
IZ	X2–CZ–X2

Table II | Gate operations for parity readout. List of operations required for a complete state tomography via parity readout, with each row representing the projection axis of interest for a two-qubit system, and the sequence of gate operations required prior to readout.